Sequential Detection for a Target in Compound-Gaussian Clutter

Jian Wang and *Arye Nehorai*
Department of Electrical and Systems Engineering, Washington University in St. Louis
Bryan 201, Box 1127, 1 Brookings Drive, St. Louis, MO 63130, USA

***Abstract*— Sequential detection allows analyzing an incoming data flow, and detect the distribution change of these measurements. In this paper, we develop the sequential detection algorithm for a target under compound-Gaussian clutter. Both the target and clutter parameters are assumed unknown. We first derive the estimates for these parameters, then discuss the sequential detection algorithm for two cases: target parameter is known and unknown. We consider detections for both the target appearance and disappearance. We examine the relation between several performance measurements for the sequential detector, including the false alarm rate and the average detection delay. In the numerical example part, we first illustrate the performance of our algorithms. Then we present an example of the optimal polarimetry design in the sequential detection.**

I. Introduction

Radars are widely used to track the target and monitor the dynamically changing environment. In practice, the measurements come sequentially rather than all at once. A sequential detection procedure is used to detect the appearance or disappearance of the target based on every new incoming data. Generally, the goal of sequential detection is to detect the change-point (change in distribution) from the incoming data flow. Extensive work has been done in the past few decades. A detailed review can be found in [1] and references therein. The most common approaches in use are the Shiryaev-Roberts-Girshik-Rubin algorithm [2] which is based on Bayesian argument, and Page's cumulative sum (CUSUM) algorithm [3] which is based on the maximum likelihood. Both are known to be optimal when the observations are independently identical distributed (i.i.d.). However, one of the major disadvantages is that only one change is assumed. In [4], Tartakovsky developed an algorithm considering both the appearance and disappearance of the target.

In radar detection problem, one important thing is the modeling of clutter. As the radar resolution increases, the area of the illuminated sea surface of radar beam decreases. This causes the clutter energy fluctuating among samples. In high-resolution and low-grazing-angle radar, the real clutter data show significant deviations from the complex Gaussian model, see [5]-[9]. The received clutter contains many target-like spikes, which can increase the radar detectors' probability of false alarm. In many cases, it has been found that the sea clutter can be suitably modeled with the *compound-Gaussian* distributed random variable, see [5]-[11]. In this model, the fast-changing component, which accounts for local scattering, is referred to as *speckle* $\boldsymbol{\chi}(t)$. It is assumed to be a stationary complex Gaussian process with zero mean. The slow-changing component, *texture* $u(t)$ is used to describe the variation of the local power due to the tilting of the illuminated area, and it is modeled as a stationary positive real random process. The complex clutter can be written as the product of these two components

$$\boldsymbol{e}(t) = \sqrt{u(t)}\boldsymbol{\chi}(t). \tag{1}$$

In our previous work [12], we applied the GMANOVA model (see [13]) to the parameter estimation problem of distributed target under the compound-Gaussian clutter. We derived the maximum-likelihood (ML) estimates of the target reflection matrix, the speckle covariance matrix and the texture distribution parameter. In this paper, we extend the work in [12] for the problem of sequential detection of a target under compound-Gaussian clutter. We will consider both the cases of known and unknown target parameter. The performance of the sequential detector will also be discussed.

The paper is organized as follows. In Section II, we introduce the measurement model. In Section III, we reviewed the traditional sequential detection procedure. In section IV and V, we derived the sequential detection procedure by assuming the target parameter is known and unknown respectively. We also discussed the performance of the detectors in these two section. In Section VI, we examine our algorithm with numerical examples. Finally we conclude the work in Section VII.

II. Measurement Model

In this section, we explain the structured measurement model used. We extend the radar array measurement model in [14] to account for compound-Gaussian clutter, see also [12]. We consider a radar array with n elements and receives return from P pulses, where each pulse return provides N samples. We collect the spatio-temporal data from the tth range gate into a vector $\boldsymbol{y}(t)$ of size $m = nP$ and model $\boldsymbol{y}(t)$ as (see [13] and [14]):

$$\boldsymbol{y}(t) = AX\boldsymbol{\phi}(t) + \boldsymbol{e}(t), \quad t = 1, \ldots, N. \tag{2}$$

where A is an $m \times r$ spatio-temporal steering matrix of the targets, $\Phi = [\boldsymbol{\phi}(1), \boldsymbol{\phi}(2), \ldots, \boldsymbol{\phi}(N)]$ is the temporal response matrix, X is an $r \times d$ matrix of unknown complex amplitudes of the targets. Here r is the number of possible directions that the reflection signals will come from, and d is the number of range gate that covers the target. The additive noise vector

$\boldsymbol{e}(t), t = 1, 2, \ldots, N$ is assumed to be i.i.d. and come from a compound-Gaussian probability distribution, see e.g. [6]-[9], [15] and [16]. Note that a special case of the model (2) for rank-one targets (i.e., scalar X) under compound-Gaussian clutter was considered in [7]. Another special case is presented in [17], where the model used for optimal polarimetry design is a special case of the model (2) with rank 2 target.

We now represent the above measurement scenario using the following hierarchical statistical model: $\boldsymbol{y}(t)$ are conditionally independent random vectors with probability density functions (pdfs)

$$p_{y|u}(\boldsymbol{y}(t)\,|\,u(t); X, \Sigma) = \exp\Big\{ -[\boldsymbol{y}(t) - AX\boldsymbol{\phi}(t)]^H \cdot [u(t)\Sigma]^{-1} \cdot [\boldsymbol{y}(t) - AX\boldsymbol{\phi}(t)]\Big\} \Big/ |\pi u(t)\Sigma|, \quad (3)$$

where the superscript "^{H}" denotes the Hermitian (conjugate) transpose, Σ is the (unknown) covariance matrix of the speckle component, and $u(t), t = 1, 2, \ldots, N$ are the unobserved texture components (powers). We assume $u(t)$ follows the inverse gamma texture distribution because of the simplicity in its computation, see [18], [19], and [20]. It has been shown to fit well real data in [20].

By definition, the reciprocal of $u(t)$ follows a gamma distribution with mean one and unknown shape parameter ν, i.e. the probability density function (pdf) of $u(t)$ is

$$p_u(u(t); \nu) = \frac{1}{\Gamma(\nu)} \nu^\nu u(t)^{-\nu-1} e^{-\nu/u(t)} \sim \text{iGamma}(\nu, 1/\nu), \quad (4)$$

where $\Gamma(\cdot)$ is the gamma function. The conditional distribution of $\boldsymbol{y}(t)$ given $u(t)$ is

$$p_{y|u}(\boldsymbol{y}(t)\,|\,u(t); X, \Sigma) = \exp\Big\{ -[\boldsymbol{y}(t) - AX\boldsymbol{\phi}(t)]^H \cdot [u(t)\Sigma]^{-1} \cdot [\boldsymbol{y}(t) - AX\boldsymbol{\phi}(t)]\Big\} \Big/ |\pi u(t)\Sigma|. \quad (5)$$

Integrating out the unobserved data $u(t)$, we obtain a *closed-form* expression for the marginal pdf of $\boldsymbol{y}(t)$:

$$p_y(\boldsymbol{y}(t); X, \Sigma, \nu) = \frac{\Gamma(\nu + m)}{|\pi\Sigma| \cdot \Gamma(\nu) \cdot \nu^m} \cdot \Big\{1 + [\boldsymbol{y}(t) - AX\boldsymbol{\phi}(t)]^H \Sigma^{-1} [\boldsymbol{y}(t) - AX\boldsymbol{\phi}(t)]/\nu\Big\}^{-\nu-m}. \quad (6)$$

III. Review of Sequential Detection

In this section we review a frame work of detecting the appearance and disappearance of a target under compound-Gaussian clutter background using sequential detection. The sequential detection problem can be expressed in the language of hypothesis of the following form:

$H_{\lambda,\gamma}$: "target appears at time λ and disappears at γ", $1 \le \lambda \le N, \gamma \ge \lambda + 1$;

H_0 : "the target does not appear",

where the alternative hypothesis $H_{\lambda,\gamma}$ is the hypothesis that the target appears at $\lambda \in \{1, 2, \ldots, N\}$ and disappears at $\gamma > \lambda$ while the null hypothesis H_0 represents that the target does not appear during the observation interval. In our problem, we assume each measurement is i.i.d..

Denote by $\boldsymbol{\theta}_0 = \{\Sigma, \nu\}$ and $\boldsymbol{\theta}_1 = \{X, \Sigma, \nu\} = \{X, \boldsymbol{\theta}_0\}$ the parameter sets under H_1 and H_0 respectively. The likelihood ratio based on the observed data $Y_N = [\boldsymbol{y}(1), \boldsymbol{y}(2), \ldots, \boldsymbol{y}(N)]$ can be expressed as

$$\Lambda_{N,\lambda,\gamma}(\boldsymbol{\theta}_1, \boldsymbol{\theta}_0) = \frac{p(Y_N|H_{\lambda,\gamma})}{p(Y_N|H_0)} = \prod_{t=\lambda}^{\gamma} \frac{p_1(\boldsymbol{y}(t); \boldsymbol{\theta}_1)}{p_0(\boldsymbol{y}(t); \boldsymbol{\theta}_0)}. \quad (7)$$

The generalized log-likelihood ratio (GLR) statistic L_N can be written as

$$L_N = \ln \max_{\lambda,\gamma} \Lambda_{N,\lambda,\gamma}(\boldsymbol{\theta}_1, \boldsymbol{\theta}_0) = \max_{\substack{1 \le \lambda \le N \\ \gamma \ge \lambda+1}} \sum_{t=\lambda}^{\gamma} \ell_t(\boldsymbol{\theta}_1, \boldsymbol{\theta}_0), \quad (8)$$

where

$$\ell_t(\boldsymbol{\theta}_1, \boldsymbol{\theta}_0) = \ln \frac{p_1(\boldsymbol{y}(t); \boldsymbol{\theta}_1)}{p_0(\boldsymbol{y}(t); \boldsymbol{\theta}_0)}. \quad (9)$$

The GLR L_t can be written into the following recursive form [4]

$$L_t = \max\{L_{t-1}, U_t\} = \max\{U_1, U_2, \ldots, U_t\}; \quad (10a)$$

$$U_t = \ell_t(\boldsymbol{\theta}_0, \boldsymbol{\theta}_1) + \max\{0, U_{t-1}\}, \quad t \ge 1 \quad (10b)$$

with initial condition $L_0 = U_0 = 0$.

In sequential detection, the GLR $L_t, t = 1, 2, \ldots, N$ is calculated and compared with threshold η_a every time when new data $\boldsymbol{y}(t)$ is available. The decision on target appearance is made once L_t exceeds the threshold. Recall (10b), the stopping time τ_a for detection of the appearance of the target can be written as

$$\tau_a = \min\{t : U_t \ge \eta_a\}, \quad \text{or} \quad \tau_a = \min\{t : L_t \ge \eta_a\}, \quad (11)$$

which is known as the CUSUM procedure.

It is straightforward to decide the target's disappearance if U_t goes below η_a after exceedance. The drawback of this algorithm is that it can control either the false alarm rate and false detection rate of the target's disappearance, but not both. In [4], the author propose an algorithm to detect the disappearance of the target after making the decision that the target appears. We ignore the derivation and present the algorithm here:

1) If the decision "target appears" is made at time τ_a, the data up to τ_a are discarded.
2) Recalculate L_t and U_t whenever new data comes in. The decision "target disappears" is made when

$$L_t - U_t > \eta_d \quad (12)$$

where η_d is a threshold for target disappearing.

IV. Sequential Detection Under Compound-Gaussian Clutter, Case I: Known Target Parameter

In this section, we will apply the CUSUM sequential detection procedure to our problem for distributed target detection in compound-Gaussian clutter. We consider the case that the

target parameter X is known. We first present the parameter estimation algorithms in Section IV-A. Then we propose a sequential detection algorithm in Section IV-B. At the end of this section, we analyze the performance of our detector. The case of unknown X will be considered in Section V.

A. Preliminary Parameters Estimation

We assume the sea clutter is consistent during the observation, i.e., the clutter distribution parameters Σ and ν are unchanged in the whole process. We also assume enough secondary data, including both pure clutter data and the mixture data of clutter and signal, is available before the detection process. We now first estimate Σ and ν from the secondary data.

It is obvious from (6) that the pure clutter signal $\boldsymbol{y}(t) = \boldsymbol{e}(t)$ has the marginal pdf

$$p_0(\boldsymbol{y}(t);\Sigma,\nu) = \frac{\Gamma\big(\nu+m\big)}{|\pi\Sigma|\cdot\Gamma\big(\nu\big)\cdot\nu^m}\cdot\Big\{1+\boldsymbol{y}(t)^H\,\Sigma^{-1}\,\boldsymbol{y}(t)/\nu\Big\}^{-\nu-m} \quad (13)$$

It is impossible to get a closed-form solution for the estimates of Σ and ν. In [12], we derived an algorithm based on parameter-expanded expectation-maximization (PX-EM) method to jointly estimate both the target and clutter parameter. To estimate only the clutter parameter, we can still use that algorithm with minor modifications. Because of the length limit, we do not present it here.

Once the clutter parameters are determined, the pdf of the measurement data $\boldsymbol{y}(t)$ under alternative hypothesis can be written as (see also (6))

$$p_1(\boldsymbol{y}(t);X,\widehat{\Sigma},\widehat{\nu}) = \frac{\Gamma\big(\widehat{\nu}+m\big)}{|\pi\widehat{\Sigma}|\cdot\Gamma\big(\widehat{\nu}\big)\cdot\widehat{\nu}^m}$$
$$\cdot\Big\{1+[\boldsymbol{y}(t)-AX\boldsymbol{\phi}(t)]^H\,\widehat{\Sigma}^{-1}\,[\boldsymbol{y}(t)-AX\boldsymbol{\phi}(t)]/\widehat{\nu}\Big\}^{-\widehat{\nu}-m}, \quad t=\lambda,\lambda+1,\ldots \quad (14)$$

where $\widehat{\Sigma}$ and $\widehat{\nu}$ are estimates of clutter parameters derived from secondary data. Similarly, we use the modified PX-EM algorithm to estimate the unknown target parameter X.

Here we modify the joint estimation algorithm in [12] into two separate parts just for the convenience of following procedures.

B. Sequential Detection Process

Under the assumption that the target is absent at the beginning of the observation, our algorithm need to detect two change-points: the target's appearance and disappearance. After that, the system is reset and new observation cycle begins.

Target appearance detection: with the knowledge of both clutter and target parameters, we take following steps to detect the target's appearance when the new measurement is available

1) Compute the likelihood of $\boldsymbol{y}(t)$ under the null hypothesis $p_0(\boldsymbol{y}(t);\widehat{\Sigma},\widehat{\nu})$ with (13).
2) Compute the likelihood of $\boldsymbol{y}(t)$ under the alternate hypothesis $p_1(\boldsymbol{y}(t);\widehat{X},\widehat{\Sigma},\widehat{\nu})$ with (14).
3) Compute the log-likelihood of the current observation $\ell_t(\widehat{X},\widehat{\Sigma},\widehat{\nu})$ with (9). Update L_t and U_t with (10).
4) Decide "target appears" if and only if $U_t \geq \eta_a$ or $L_t \geq \eta_a$. The appearance time $\tau_a = t$.

Target disappearance detection: if the decision "target appears" is made, the observation counter is set to zero and we assume the target exists until the first time it disappears. The algorithm is symmetric to the one for target appearance:

1) Compute the likelihood $p_1(\boldsymbol{y}(t);\widehat{X},\widehat{\Sigma},\widehat{\nu})$ with (14).
2) Compute $p_0(\boldsymbol{y}(t);\widehat{\Sigma},\widehat{\nu})$ with (13).
3) Compute the log-likelihood of the current observation $\ell_t(\widehat{X},\widehat{\Sigma},\widehat{\nu})$ with (9). Then update L_t and U_t with (10).
4) Decide "target disappears" if and only if $L_t - U_t < \eta_d$. The disappearance time $\tau_d = \tau_a + t$.

C. Performance Analysis

Usually the performance of sequential detection algorithms are evaluated by two indices: the false alarm rate (frequency of false alarms, P_{FA}) and the average detection delay (ADD). A detector with smaller ADD, i.e., more sensitive to the distribution change of the dataflow, will have higher false alarm rate, and vice versa. The optimal detector design will involve a trade-off between these two measurements.

In the following, we first compute ADD for the sequential detector. Then we discuss the properties of these two performance measurements.

1) Average Detection Delay: An important performance of target detection is average detection delay (ADD), which is also known as the average sample number (see [21, Ch. 9]). Different detectors have different ADD. With the same false alarm rate P_{FA}, the smaller ADD the better is the algorithm.

We now calculate the ADD for the target appearance. After the appearance of the target, each new measurement will increase the general likelihood ratio, see (8), until the accumulation overpass the threshold and trigger the detector. With some approximations, we proved that before the appearance of target,

$$\mathrm{E}_0[U_t|H_0] \approx 0.$$

After target appearance, the statistic U_t will increase when each new measurement comes. The expectation of this increase is:

$$\mathrm{E}_1[\ell_t|H_0] = (-\nu-m)\frac{\int_0^\infty \ln(1+\frac{r^2}{\nu})(1+\frac{r^2}{\nu})^{-\nu-m}r^{2m-1}dr}{\int_0^\infty(1+\frac{r^2}{\nu})^{-\nu-m}r^{2m-1}dr}$$
$$+(\nu+m)\frac{\int_0^\infty \ln(1+\frac{r^2}{\nu}+K)(1+\frac{r^2}{\nu})^{-\nu-m}r^{2m-1}dr}{\int_0^\infty(1+\frac{r^2}{\nu})^{-\nu-m}r^{2m-1}dr}, \quad (15)$$

where

$$K = \frac{[AX\boldsymbol{\phi}(t)]^H\Sigma^{-1}[AX\boldsymbol{\phi}(t)]}{\nu}. \quad (16)$$

The integrals in the numerator and denominator of (15) are efficiently and accurately evaluated using the generalized

Gauss-Laguerre quadrature formula (see [22, Ch. 5.3]):

$$\int_0^\infty f(x)\cdot x^{k-1}\exp(-x)\,dx \approx \sum_{l=1}^{L} w_l(k-1)\,f(x_l(k-1)), \tag{17}$$

where $f(x)$ is an arbitrary real function, L is the quadrature order, and $x_l(k-1)$ and $w_l(k-1)$, $l=1,2,\ldots,L$ are the abscissas and weights of the generalized Gauss-Laguerre quadrature with parameter $k-1$.

The ADD for detection can be approximately calculated as below

$$\mathrm{ADD} = \eta_a / \mathrm{E}_1[\ell_t|H_0] \tag{18}$$

2) False Alarm Rate and Threshold: The false alarm of our sequential detector include two aspects: false alarm for target appearance and disappearance. Since they are symmetric, we only derive the false alarm for target appearance here.

A straightforward way to determine the threshold η_a given a false alarm rate is to use Monte-Carlo simulation under H_0. The number of simulations and computation load are usually huge due to the small value of P_{FA}. In [4], a simple lower bound for the threshold for a given false alarm rate is derived:

$$\eta_a = \ln(N_{\mathrm{tar}}/P_{\mathrm{FA}}), \tag{19}$$

where N_{tar} is the maximum number of targets, which equals to 1 in our case.

V. Sequential Detection Under Compound-Gaussian Clutter, Case II: Unknown Target Parameter

When both target parameter and change time τ_a are unknown, the detection procedure is closely interrelated with the estimation problem. This case is very possible in practice, and it is known that this problem is much harder to solve [23]. Usually CUSUM algorithm can be used for *known* values of X to detect the unknown time of change and Kalman filter can be use to estimate X for a known value of τ_a. When both are known, the problem cannot be solved properly.

In this section, we consider the case where both the target parameter X and the change time λ and γ are unknown. To solve this problem, we consider a sub-optimal method. We first propose a sub-optimal estimate of the target parameter X, then substitute this estimate into the statistics L_N and U_N to detect the appearance and disappearance of the target.

A. Target Appearance Detection

Assume the target appears at time instant λ, $1\le\lambda\le N$. The generalized log-likelihood ratio statistic L_N can be written as (see (8) and (9))

$$L_N = \max_{1\le\lambda\le N}\max_{X}\sum_{t=\lambda}^{N}\ln\frac{p_1(\boldsymbol{y}(t);X,\Sigma,\nu)}{p_0(\boldsymbol{y}(t);\Sigma,\nu)}. \tag{20}$$

Substitute (13) and (14) into above equation, it is easy to obtain

$$L_N = \max_{1\le\lambda\le N}\max_{X}(-\nu-m) \cdot\sum_{t=\lambda}^{N}\ln\Big\{\frac{1+[\boldsymbol{y}(t)-AX\boldsymbol{\phi}(t)]^H\Sigma^{-1}[\boldsymbol{y}(t)-AX\boldsymbol{\phi}(t)]/\nu}{1+\boldsymbol{y}(t)^H\Sigma^{-1}\boldsymbol{y}(t)/\nu}\Big\}. \tag{21}$$

In the above expression, X is the ML estimate by assuming target appears at $t=\lambda$ and exists till $t=N$, i.e., the estimate minimizing $\sum_{t=\lambda}^{N}\ln\Big\{1+[\boldsymbol{y}(t)-AX\boldsymbol{\phi}(t)]^H\Sigma^{-1}[\boldsymbol{y}(t)-AX\boldsymbol{\phi}(t)]/\nu\Big\}$. We have derived the ML estimate of X. However, the EM algorithm requires at least tens of measurements to converge, which is impossible when $N-\lambda$ is small. Hence we propose another estimate for X.

Since $\ln(\cdot)$ is a concave function, it is straightforward to obtain:

$$\sum_{t=\lambda}^{N}\ln\Big\{1+[\boldsymbol{y}(t)-AX\boldsymbol{\phi}(t)]^H\Sigma^{-1}[\boldsymbol{y}(t)-AX\boldsymbol{\phi}(t)]/\nu\Big\} \le (N-\lambda+1)\ln\Big\{\frac{1}{N-\lambda+1} \cdot\sum_{t=\lambda}^{N}\big\{1+[\boldsymbol{y}(t)-AX\boldsymbol{\phi}(t)]^H\Sigma^{-1}[\boldsymbol{y}(t)-AX\boldsymbol{\phi}(t)]/\nu\big\}\Big\}.$$

We now seek the estimate $\widetilde{X}$ which minimizes the right hand side of the above inequality, which is the upper bound of $\sum_{t=\lambda}^{N}\ln\Big\{1+[\boldsymbol{y}(t)-AX\boldsymbol{\phi}(t)]^H\Sigma^{-1}[\boldsymbol{y}(t)-AX\boldsymbol{\phi}(t)]/\nu\Big\}$. After simplification, the estimate can be written as

$$\widetilde{X} = \arg\min_{X}\sum_{t=\lambda}^{N}[\boldsymbol{y}(t)-AX\boldsymbol{\phi}(t)]^H\Sigma^{-1}[\boldsymbol{y}(t)-AX\boldsymbol{\phi}(t)]. \tag{22}$$

The closed-form solution of $\widetilde{X}$ is derived as below:

$$\mathrm{vec}(\widetilde{X}) = \Big[\sum_{t=\lambda}^{N}(\boldsymbol{\phi}(t)^T\otimes A)^H\Sigma^{-1}(\boldsymbol{\phi}(t)^T\otimes A)\Big]^{-1} \cdot\Big[\sum_{t=\lambda}^{N}\boldsymbol{y}(t)^H\Sigma^{-1}(\boldsymbol{\phi}(t)^T\otimes A)\Big]^H, \tag{23}$$

where "vec$(\cdot)$" is the vectorizing operator which stack the columns of a matrix, and "$\otimes$" denotes the Kronecker product. In practice, the matrix $\sum_{t=\lambda}^{N}(\boldsymbol{\phi}(t)^T\otimes A)^H\Sigma^{-1}(\boldsymbol{\phi}(t)^T\otimes A)$ could be singular. We revise (23) as below

$$\mathrm{vec}(\widetilde{X}) = \Big[\sum_{t=\lambda}^{N}(\boldsymbol{\phi}(t)^T\otimes A)^H\Sigma^{-1}(\boldsymbol{\phi}(t)^T\otimes A)+\epsilon I\Big]^{-1} \cdot\Big[\sum_{t=\lambda}^{N}\boldsymbol{y}(t)^H\Sigma^{-1}(\boldsymbol{\phi}(t)^T\otimes A)\Big]^H, \tag{24}$$

where ϵ is a tiny positive number and I is an identity matrix with appropriate dimension.

Hence the target appearance detection procedure can be summarized as follows:

1) For every incoming new measurement $\boldsymbol{y}(N)$, compute the statistic L_N with (21), where the target parameter X can be estimated using (24).
2) Decide "target appears" if and only if $L_N \geq \eta_a$. The appearance time $\tau_a = N$.

B. Target Disappearance Detection

Once the target is detected, the measurement counter is set to zero. Both L_0 and U_0 are initialized with the value surpassing the target appearance threshold. The target parameter X is initialized with the last estimate in the phase of target appearance detection. For every new incoming measurement, if it is determined containing target information, we use it to update the X value followed by L_t and U_t. The target disappearance detection procedure is almost same with the one described in Section IV.

C. Performance Analysis

In Section IV-C, we discussed the ADD, the relation between false alarm rate and the threshold for sequential detector. Since we assumed the full information of the target parameter in the discussion, all the results can be viewed as in ideal case and the benchmarks for performance evaluation.

VI. Numerical Examples

In this section, we examine the algorithms we developed in Section IV and V with two numerical examples.

A. Example 1: Comparison of Sequential Detectors: Known and Unknown X Cases

To examine the detectors we presented in Section IV and V, we use the measurement scenario similar to the one used in [12]. The radar array include $n = 2$ elements and transmits $P = 2$ pulses, implying that $m = 4$. We select a rank-one target scenario with $\boldsymbol{\phi}(t) = 1, t = 1, 2, \ldots, N$, complex target amplitude $X = 0.207 \cdot \exp(j\pi/7)$, and

$$A = \boldsymbol{b}(\varpi) \otimes \boldsymbol{a}(\vartheta), \tag{25}$$

where $\boldsymbol{b}(\varpi) = [1, \exp(j2\pi\varpi), \exp(j4\pi\varpi)]^T$ with normalized Doppler frequency $\varpi = 0.42$, and $\boldsymbol{a}(\vartheta) = [1, \exp(j2\pi\vartheta), \exp(j4\pi\vartheta)]^T$ with spatial frequency $\vartheta = 0.926$. The speckle covariance matrix Σ was generated using a model similar to that in [24, Sec. 2.6] with 1000 patches. The (p, q)th element of the covariance matrix of the speckle component was chosen as

$$\Sigma_{p,q} = \sigma^2 \cdot 0.9^{|p-q|} \cdot \exp[j(\pi/2)(p-q)], \tag{26}$$

which is the correlated noise covariance model used in [25] (see also references therein). In the simulations presented here, we select $\sigma^2 = 10.17$. The target appears at $t = 50$ and disappears at $t = 100$. Totally $N = 150$ samples are received. When calculating the ADD, we set the order of the generalized Gauss-Laguerre quadratures to $L = 30$.

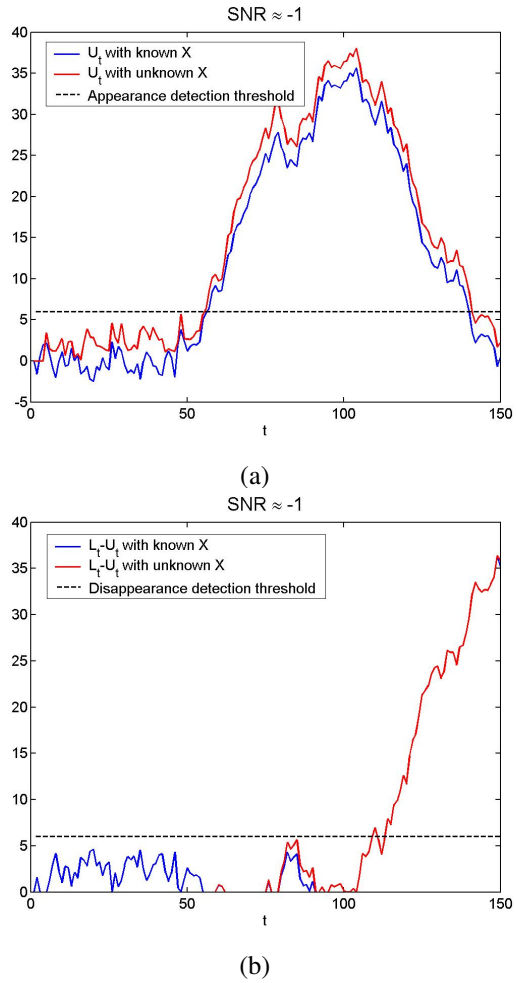

Fig. 1. Detection of target's appearance and disappearance. Target appears at $t = 50$ and disappears at $t = 100$. (a) Target appearance detection: U_t as a function of t, with known and unknown X. (b) Target disappearance detection: $L_t - U_t$ as a function of t, with known and unknown X.

In Fig. 1, we compare the performance of the algorithm for known and unknown X. The results show that without the knowledge of X, our algorithm can also has a comparable performance with the algorithm for known X. Note that in Fig. 1(b). The curves of both cases overlap each other after detection. The signal-to-noise ratio (SNR) in the above example is approximately -1 dB.

In Fig. 2, we illustrate the ADDs as a function of the false alarm rate. The theoretical ADD is calculated with (15), (18) and (19). The ADDs of known and unknown X are averaged over 30 simulation results for each P_{FA}. Note we only consider the appearance detection here. It is obvious that the ADDs of our algorithms developed in Section IV and V approximate the theoretical one as P_{FA} becoming smaller, i.e., the threshold η_a becoming higher. When P_{FA} is big, the ADD with unknown X deviates from the theoretical prediction severely. It is even below zero when P_{FA} is greater than 0.05 approximately, which means the detector "detects" the target before it appears, i.e., false alarm. We need to adjust

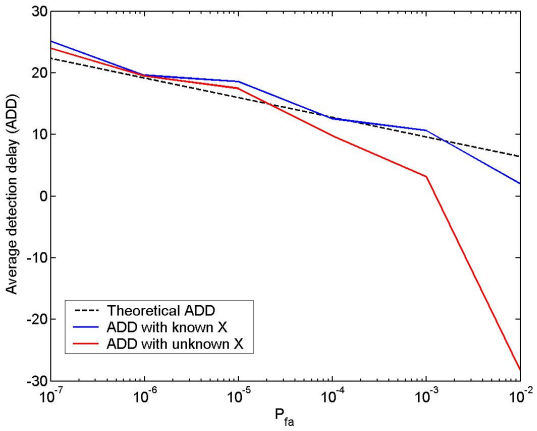

Fig. 2. Average detection delay (ADD) as a function of false alarm rate (P_{FA}).

the threshold value of the detection when the target parameter X is unknown in practice. Interestingly, we notice that the ADDs with unknown X is uniformly smaller than the ones with known X. This is because that for a given set of data, the model with more unknown parameters has a larger likelihood, see also Fig. 1(a). This is also the reason why the algorithm with unknown X has a higher P_{FA} compared with the one with unknown X.

B. Example 2: Optimal Polarimetry Design

We examine our algorithms through the polarimetry design problem. For simplicity, we assume the target may appear in an area with known range and azimuth angle during the observation. Here we follow the notations in [17]. Let $\boldsymbol{\xi}(t) = [\xi_{\mathrm{h}}(t), \xi_v(t)]^T$ be the transmitted (incident) polarized electric field impinging on the target, and $\boldsymbol{y}(t) = [y_{\mathrm{h}}(t), y_v(t)]^T$ be the complex envelope of the received (scattered) electric field, where the subscripts "h" and "v" denote the horizontal and vertical polarization components of a fully polarized signal. Under the far-field assumption, the scattered field is related to the incident field by [26], [27], [28]

$$\boldsymbol{y}(t) = g(r)\, S\, \boldsymbol{\xi}(t) + \boldsymbol{e}(t), \quad t = 1, 2, \ldots, N, \tag{27}$$

where r denotes the range from the transmitting antenna to the target, S is the 2×2 scattering matrix, and $\boldsymbol{e}(t)$ denotes additive clutter. Assume $\boldsymbol{e}(t) = [e_{\mathrm{h}}(t), e_v(t)]^T$ to be i.i.d., under compound-Gaussian with parameters Σ and ν, where the superscript "T" denotes the (non-conjugate) transpose. The variable N is the number of temporal observations. Denoting the wave number of the carrier waveform by k, we have $g(r) = e^{-2jkr}/2kr$ corresponding to the propagation magnitude attenuation and phase shift, which is a (known) complex scalar.

Note that measurement model (27) is a direct application of model (2) by letting $A = g(r) \cdot I$, $X = S$ and $\boldsymbol{\phi}(t) = \boldsymbol{\xi}(t)$.

We parameterize the transmitted polarized signal using the notations of [29] and [30] (omitting time index for notational simplicity):

$$\boldsymbol{\xi} = \|\boldsymbol{\xi}\| e^{j\varphi} \begin{bmatrix} \cos\alpha\cos\beta + j\sin\alpha\sin\beta \\ -\sin\alpha\cos\beta + j\cos\alpha\sin\beta \end{bmatrix} \tag{28}$$

where $\|\boldsymbol{\xi}\| e^{j\varphi}$ is the complex envelope of the source signal, α denotes the rotation angle between the system coordinates and the electric ellipse axes, and β determines the ellipse's eccentricity. The definition space of these parameters are: $\|\boldsymbol{\xi}\| \geq 0$, $\varphi \in (-\pi, \pi]$, $\alpha \in (-\pi/2, \pi/2]$, $\beta \in [-\pi/4, \pi/4]$. Considering that the transmitted signal is power-limited, we exclude $\|\boldsymbol{\xi}\|$ out of the design by setting $\|\boldsymbol{\xi}\| = 1$.

We set the true value of the scattering matrix to

$$S = \begin{bmatrix} 2j & 0.5 \\ 0.5 & -j \end{bmatrix}, \tag{29}$$

which is used also in [31] and [26]. The speckle covariance matrix Σ was generated using a model similar to that in [24, Sec. 2.6] with 1000 patches. The (p, q)th element of the covariance matrix of the speckle component was chosen as

$$\Sigma_{p,q} = \sigma^2 \cdot 0.9^{|p-q|} \cdot \exp[j(\pi/2)(p-q)], \quad p, q = 1, 2, \ldots, m \tag{30}$$

In the examples presented here, we selected $\sigma^2 = 2.05$. In the following numerical examples, without specification, we set the speckle covariance matrix to the above value and the texture distribution parameter $\nu = 2$. Since we assume the target's range r and direction are known, the value of factor $g(r)$ will not affect the results.

The optimal polarimetry signal is designed to minimize the ADD, which is equivalent to maximize K, see (15) and (16). The numerator of K, $[AX\boldsymbol{\phi}(t)]^H \Sigma^{-1} [AX\boldsymbol{\phi}(t)]$, denotes the energy reflected from target. We are seeking the optimal polarimetry to maximize this energy. It is easy to find that the signal phase φ does not affect the result. To find the optimal value of α and β, we search the definition space:

$$(\alpha, \beta) = \arg \max_{(\alpha,\beta) \in [-\frac{\pi}{2}, \frac{\pi}{2}) \times [-\frac{\pi}{4}, \frac{\pi}{4}]} [AX\boldsymbol{\phi}(t)]^H \Sigma^{-1} [AX\boldsymbol{\phi}(t)] \tag{31}$$

We calculate the theoretical ADD based on the parameters and the optimal signal polarimetry. To show the superiority, we show the ADD and the theoretical ADD of a reference signal. The reference signal polarimetry is set to $\alpha = \frac{\pi}{4}$ and $\beta = \frac{\pi}{6}$.

We show the results in Fig. 3. The results are averaged among 100 experiments. It is obvious that the optimal designed signal has a smaller ADD for each P_{FA}. The slope of the optimal ADD curve is also smaller than the optimal one.

VII. Conclusions

We developed radar sequential detection procedures for a target in the compound-Gaussian clutter. We consider cases where target parameter is known or not. In both cases, we assume the secondary data for compound-Gaussian clutter parameters estimation are available. We first developed the sequential detection procedure for target appearance and disappearance by applying the traditional CUSUM method to

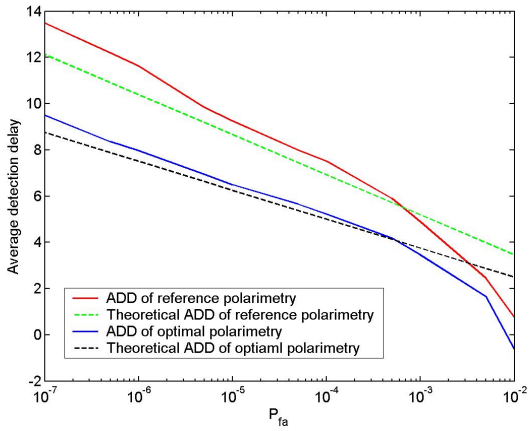

Fig. 3. Average detection delay comparison of the optimal polarimetry and a reference polarimetry.

the compound-Gaussian clutter with known target parameter. In addition, we analyzed relation between the performance measurements of sequential detectors: probability of false alarm, threshold and average detection delay. In the case where the target parameter is unknown, we first developed a adaptive sub-optimal estimate for the target parameter, then substitute this estimate back to the sequential detector. In the numerical examples, we compared the performance of sequential detector with and without the knowledge of the target parameter. We also applied our results to an optimal waveform design problem to minimize the average detection delay.

REFERENCES

[1] T. Lai, "Sequential analysis: some classical problems and chanllenges," *Statistica Sinica*, vol. 11, pp. 303-408, 2001.

[2] M. Pollack, "Optimal Detection of a change in distribution," *Annal. of Statistics*, vol. 13, pp. 206-227, 1986.

[3] G. Lorden, "Procedures for reacting to a change in distribution," *Annal. of Statistics*, vol. 42, pp. 1897-1908, 1971.

[4] A. Tartakovsky, S. Kligys, and A. Petrov, "Adaptative sequential algorithms for detecting targets in a heavy IR clutter," in *SPIE Proceedings: Signal and Data Processing of Small Targets*, vol. 3809. Denver, CO, 1999.

[5] F. Gini, M. V. Greco, M. Diani, and L. Verrazzani, "Performance analysis of two adaptive radar detectors against non-Gaussian real sea clutter data," *IEEE Trans. Aerosp. Electron. Syst.*, vol. 36, pp. 1429-1439, Oct. 2000.

[6] V. Anastassopoulos, G. A. Lampropoulos, A. Drosopoulos, and N. Rey, "High resolution radar clutter statistics," *IEEE Trans. Aerosp. Electron. Syst.*, vol. 35, pp. 43-60, Jan. 1999.

[7] M. Rangaswamy and J. H. Michels, "Adaptive signal processing in non-Gaussian noise backgrounds," in *Proc. 9th IEEE SSAP Workshop,* Portland, OR, Sept. 1998, pp. 53-56.

[8] M. Rangaswamy, J. H. Michels, and B. Himed, "Statistical analysis of the nonhomogeneity detector for non-Gaussian interference backgrounds," *Proc. IEEE Radar Conf.*, Long Beach, CA, Apr. 2002, pp. 304-310.

[9] M. Rangaswamy, D. D. Weiner, and A. Ozturk, "Non-Gaussian random vector identification using spherically invariant random processes," *IEEE Trans. Aerosp. Electron. Syst.*, vol. 29, pp. 111-123, Jan. 1993.

[10] M. Greco, F. Bordoni, and F. Gini, "X-band sea-clutter nonstationarity: Influence of long waves," *IEEE Journal of Oceanic Engineering*, vol. 29, No. 2, pp. 269-283, Apr. 2004.

[11] E. Jakeman and P. N. Pusey, "A model for non-Rayleigh sea echo," *IEEE Trans. Antennas and Propagation,* vol. 24, no. 6, pp. 806-814, Nov. 1976.

[12] J. Wang, A. Dogandžić, and A. Nehorai, "Maximum likelihood estimation of compound-Gaussian clutter and target parameters," to appear in *IEEE Trans. Signal Process.*.

[13] A. Dogandžić and A. Nehorai, "Generalized multivariate analysis of variance: A unified framework for signal processing in correlated noise," *IEEE Signal Processing Mag.,* vol. 20, pp. 39–54, Sept. 2003.

[14] E. J. Kelly and K. M. Forsythe, *Adaptive detection and parameter estimation for multidimensional signal models*, Lincoln Laboratory, Tech. Report 848, April 1989.

[15] K. J. Sangston and K. R. Gerlach, "Coherent detection of radar targets in a non-Gaussian background," *IEEE Trans, on Aerospace and Electronic Systems,* vol. 30, pp. 330-340, April 1994.

[16] K. Yao, "Spherically invariant random processes: Theory and applications," in *Communications, Information and Network Security,* V.K. Bhargava *et al.*, Eds., Dordrecht, the Netherlands: Kluwer Academic Publishers, pp. 315-332, 2002.

[17] J. Wang and A. Nehorai, "Adaptive polarimetry design for a target in compound-Gaussian clutter," in revision for *IEEE Trans. Aerosp. Electron. Syst.*.

[18] A. Dogandžić, A. Nehorai, and J. Wang, "Maximum likelihood estimation of compound-Gaussian clutter and target parameters," in *Proc. 12th Ann. Workshop Adaptive Sensor Array Processing (ASAP '04)*, Lincoln Laboratory, Lexington, MA, Mar. 2004.

[19] J. Wang, A. Dogandžić, and A. Nehorai, "Cramer-Rao bounds for compound-Gaussian clutter and target parameters," *IEEE Int. Conf. Acoust., Speech, Signal Processing,* Philadelphia, PA, Mar. 2005. pp. 1101-1104.

[20] A. Balleri, A. Nehorai, and J. Wang, "Maximum likelihood estimation for compound-Gaussian clutter with inverse gamma texture," in revision for *IEEE Trans. Aerosp. Electron. Syst.*.

[21] C. W. Helstrom, *Elements of Signal Detection and Estimation*, PTR Prentice Hall, Englewood Cliffs, NJ, 1995.

[22] R.A. Thisted, *Elements of Statistical Computing: Numerical Computation*, New York: Chapman & Hall, 1988.

[23] M. H. Vellekoop and J. M. C. Clark, "A nonlinear filtering approach to change point detection problems: direct and differental-geometric methods," *Societry for Industrial and Applied Mathematics (SIAM) Review*, vol.48, No. 2, pp. 329-356, June 2006.

[24] J. Ward, *Space-Time Adaptive Processing for Airborne Radar,* Lincoln Lab., Tech. Report 1015, MIT, Dec, 1994.

[25] M. Viberg, P. Stoica, and B. Ottersten, "Maximum likelihood array processing in spatially correlated noise fields using parameterized signals," *IEEE Trans. Signal Processing,* vol. 45, pp. 996–1004, Apr. 1997.

[26] W.-M. Boerner, W. Yan, A. Xi, and Y. Ymaguchi, "On the basic pinciples of radar polarimetry: the target characteristic polarization state theory of Kennaugh, Huynen's polarization form concept, and its extension to the partially polarized case," *Proc. IEEE*, vol. 79, No. 10, pp. 1538-1550, Oct. 1991.

[27] W. M. Steedly, and R. L. Moses, "High resolution exponential modeling of fully polarized radar returns," *IEEE Trans. Aerospce Electronic Systems,* vol. 27, No. 3, pp. 459-469, May 1991.

[28] L. C. Potter, and R. L. Moses, "Attributed scattering centers for SAR ATR," *IEEE Trans. Image Processing*, vol. 6, No. 1, pp. 79-91, Jan. 1997.

[29] A. Nehorai and E. Paldi, "Vector-sensor array processing for electromagnetic source localization," *IEEE Trans. Signal Process.*, vol. SP-42, pp. 376-398, Apr. 1994.

[30] B. Hochwald and A. Nehorai, "Polarimetric modeling and parameter estimation with applications to remote sensing," *IEEE Trans. Signal Process.*, vol. SP-43, pp. 1923-1935, Aug. 1995.

[31] A. B. Kostinski and W.-M. Boerner, "On fundations of radar polarimetry," *IEEE Antennas Propagat.*, vol. AP-34, pp. 1395-1404, Dec. 1986.